REVIEW OF THEORIES FOR BLOCKING

L. Bengtsson

European Centre for Medium
Range Weather Forecasts,
England

Seminar 1979

1. INTRODUCTION

A typical feature of the general atmospheric circulation at middle and high latitudes is a tendency to fluctuate between two rather extreme circulation patterns. This behaviour of the atmosphere is most common at the Northern Hemisphere during the winter and has been known among the meteorologists for a considerable time (e.g. Garriott (1904)). One of these two states is identified by a predominantly zonal circulation or a so-called high index circulation, the other state by a meridional or a low index circulation. The meridional circulation is often broken up in a characteristic atmospheric pattern of cut-off lows and highs. These features usually have a time scale of several days during which they affect the weather in a very dominating way. The transition from the zonal to the meridional or cellular circulation is very characteristic and follows a very typical chain of events. Fig. 1.1, showing a series of idealised 500 mb maps, illustrates the change over from a high index to a low index circulation. The break-down of the westerlies at the Northern Hemisphere usually takes place in 2 preferred regions; in the eastern part of the Pacific and in the eastern part of the Atlantic ocean. A special feature of the break-down of the westerly flow is the creation of a dominating high pressure cell; what has been called a blocking high. Due to the time-scale of the blocking high, which is of the order of several days, and to the associated substantial changes in the weather type, there has always been a great meteorological interest in the blocking phenomenon.

In the infancy of numerical weather prediction the problem of blocking was studied intensively: Rossby (1949), Yeh (1949), Namias (1947), Rex (1950a, 1950b), and Berggren et al (1949). After a period of great activity among Rossby and his associates, the interest faded away and the dynamical scientists became absorbed in short

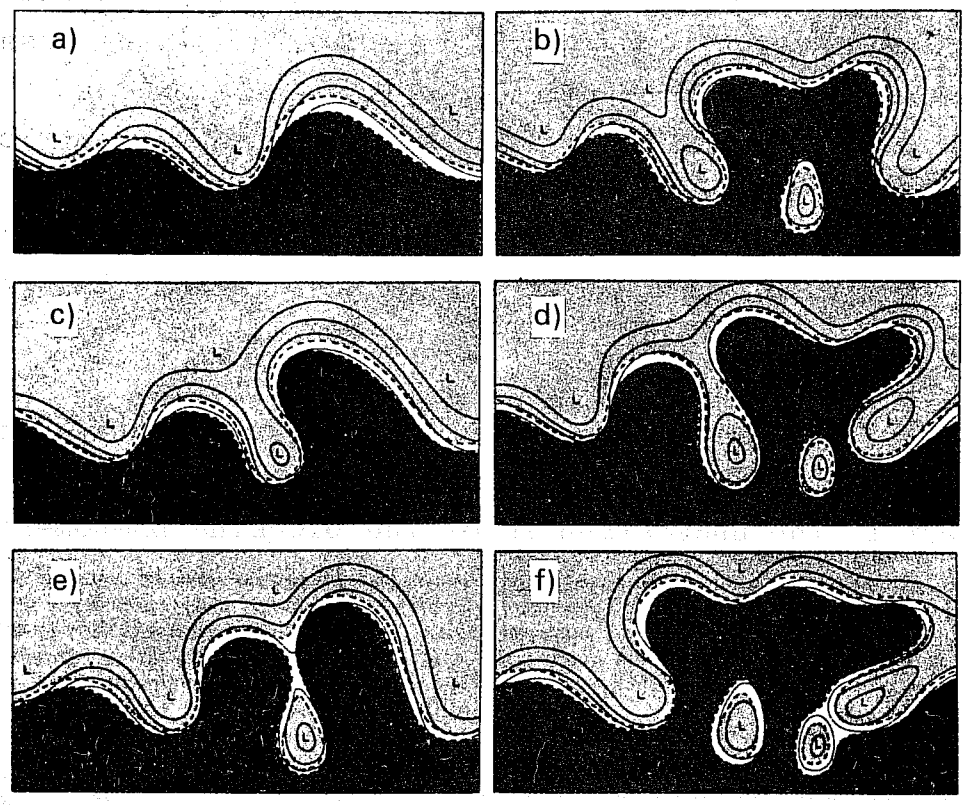

Fig. 1.1 Idealized sketches of the development of unstable waves at the 500 mb level, in association with the establishment of a blocking anticyclone in high latitudes. Cold air, light shade; warm air, dark shade. Solid lines are stream lines and broken lines the frontal surfaces (from Berggren et al, Tellus 1949).

range numerical weather prediction and the modelling of the general circulation. However, a recent interest has taken place to study the blocking phenomenon and I will here report about some new investigations carried out by Egger (1978) and Charney and DeVore (1979). From the standpoint of medium range weather forecasting the blocking phenomenon is of a fundamental interest. It is necessary to explain the physical processes essential for its generation and maintenance in order to design a numerical model for its prediction. It is also of a very great interest to investigate the phenomenon of blocking with different existing models to see to what extent blocking is predictable.

In this lecture we will present some observational material about blocking and after that discuss some theories of interest to the understanding of the blocking phenomenon. In a second lecture we will present results of some numerical models and their prospect to predict blocking

2. OBSERVATIONAL STUDIES

One of the difficulties with the study of blocking is to find a clear definition of the phenomenon itself. The definition, proposed by Rex, and given below, should be understood in the light of the theory of the hydraulic jump. This theory which we will describe in Section 4 was suggested by Rossby at the time Rex worked with Rossby at the International Meteorological Institute in Stockholm. Later empirical studies have relaxed Rex's definition and many meteorologists now understand blocking as a long lived quasi-stationary high pressure cell anomaly at middle and high latitudes.

The most comprehensive observational study of blocking has been published by Rex (1950a), (1950b). Rex suggests the following criteria for blocking. (The criteria should apply at the 500 mb level.)

(i) The basic westerly current must split into two branches.

(ii) Each branch current must transport an appreciable mass.

(iii) The double-jet system must extend over at least 45 degrees of latitude.

(iv) A sharp transition in the westerlies from a zonal type flow upstream, to a meridional type downstream must be observed across the current split.

(v) The pattern must persist with recognisable continuity for at least 10 days.

In a situation satisfying these requirements blocking is said to be initiated when (i) occurs and is said to have disappeared whenever (i), (ii), (iii) and (iv) are no longer satisfied. Using these criteria, Rex analysed the two periods 1933 - 1940 and 1945 - 1949 inclusive. The following general conclusions can be drawn.

1. The blocks have a very characteristic distribution with 2 preferred regions, one in the Atlantic area with the meridian around 10W and another one in the Pacific around 150W, Fig. 2.1. The number of cases dominates in the Atlantic but it is possible that the small number of cases in the Pacific was due to inferior data. To the knowledge of the author no comprehensive statistics of blocking are available for a later material.

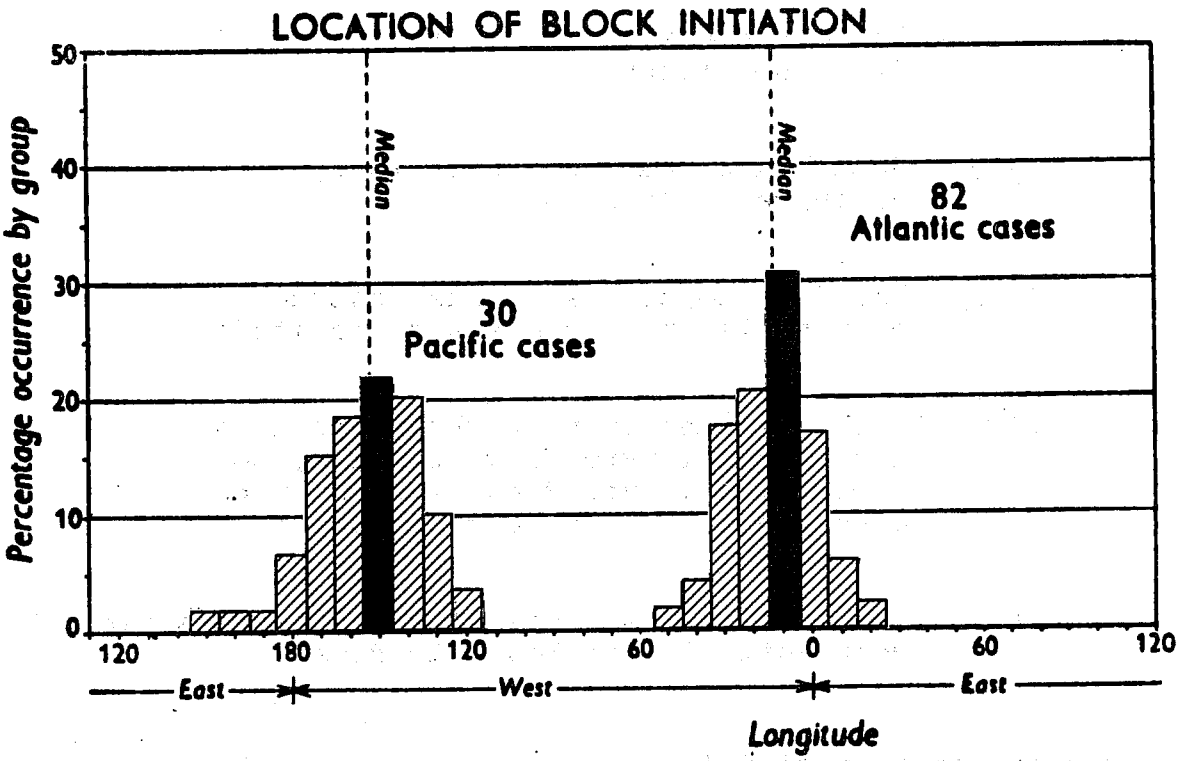

Fig. 2.1 Geographical distribution of block occurrence in the northern hemisphere; the histograms show the frequency distribution in longitude of 112 cases of block initiation at mid-tropospheric level. Modes shaded black. Cases included occurred during the years 1933 - 1940 and 1945 - 1949 inclusive (from Rex, Tellus, 1950).

2. There is a marked seasonal variation in the blocking activity as can be seen from Fig. 2.2 with a minimum around September and a maximum in April. A very marked reduction in the blocking activity occurs between May and July. There is also a substantial variation from year to year.

3. The time-scale for the blocking phenomenon is of the order of 2 weeks, Fig. 2.3. During this period the Atlantic block, which is the one most investigated, has a characteristic variation in its position. During the first phase there is a marked retrogression of the block and in the final stage an easterly movement, Fig. 2.4.

Blocking patterns, in particular well developed and long lasting ones, are most common at the Northern Hemisphere. However, they also exist at the Southern Hemisphere and according to Taljaard (1972), blocking is fairly frequent in late winter and early spring in middle latitudes, in particular in the area 135E - 160W. Other areas are around 45W (Scotia Sea, east of the Southern tip of South America) and in the vicinity of Marion and Crozet Islands (SE of South Africa). Blocking is most frequent during July - September in the south-western Atlantic and Pacific Ocean, but a secondary maximum is evident in autumn (March - May). The same seasonal variations are found in the weaker blocking area of the south-western Indian Ocean, where the two peaks are of equal magnitude.

Further, according to Taljaard the duration of the blocking is usually less than at the northern hemisphere ~ 6 days, combined with a maximum longitudinal displacement of 25^{o} during the life of the block. Taljaard further considered that the block should be centered at least 10^{o} south of the mean position of the sub-tropical high pressure belt.

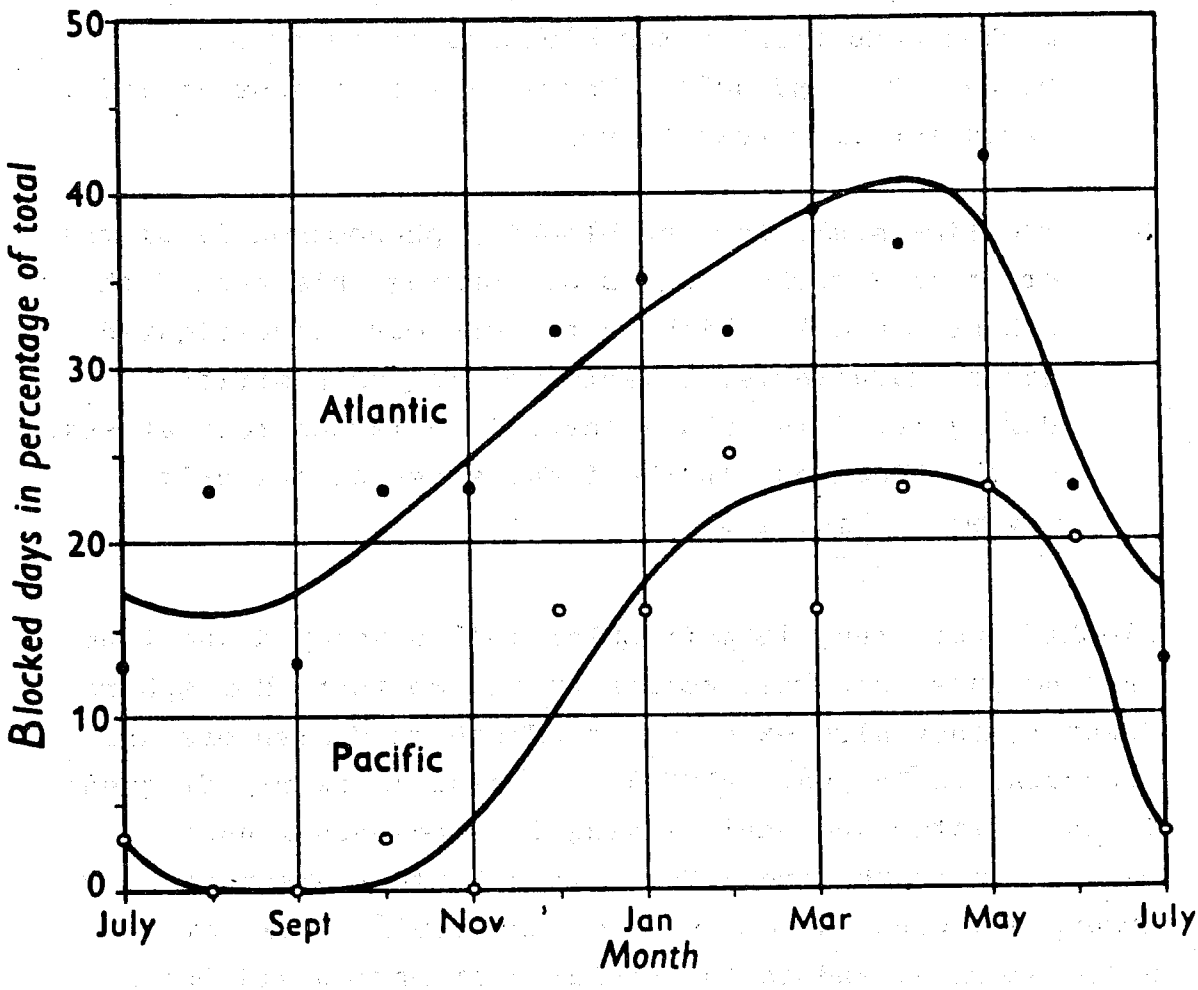

Fig. 2.2 Seasonal variation in blocking activity; Atlantic (82 cases) and Pacific (30 cases) trends in the percentage of days dominated by blocking action are shown by month (from Rex, Tellus, 1950).

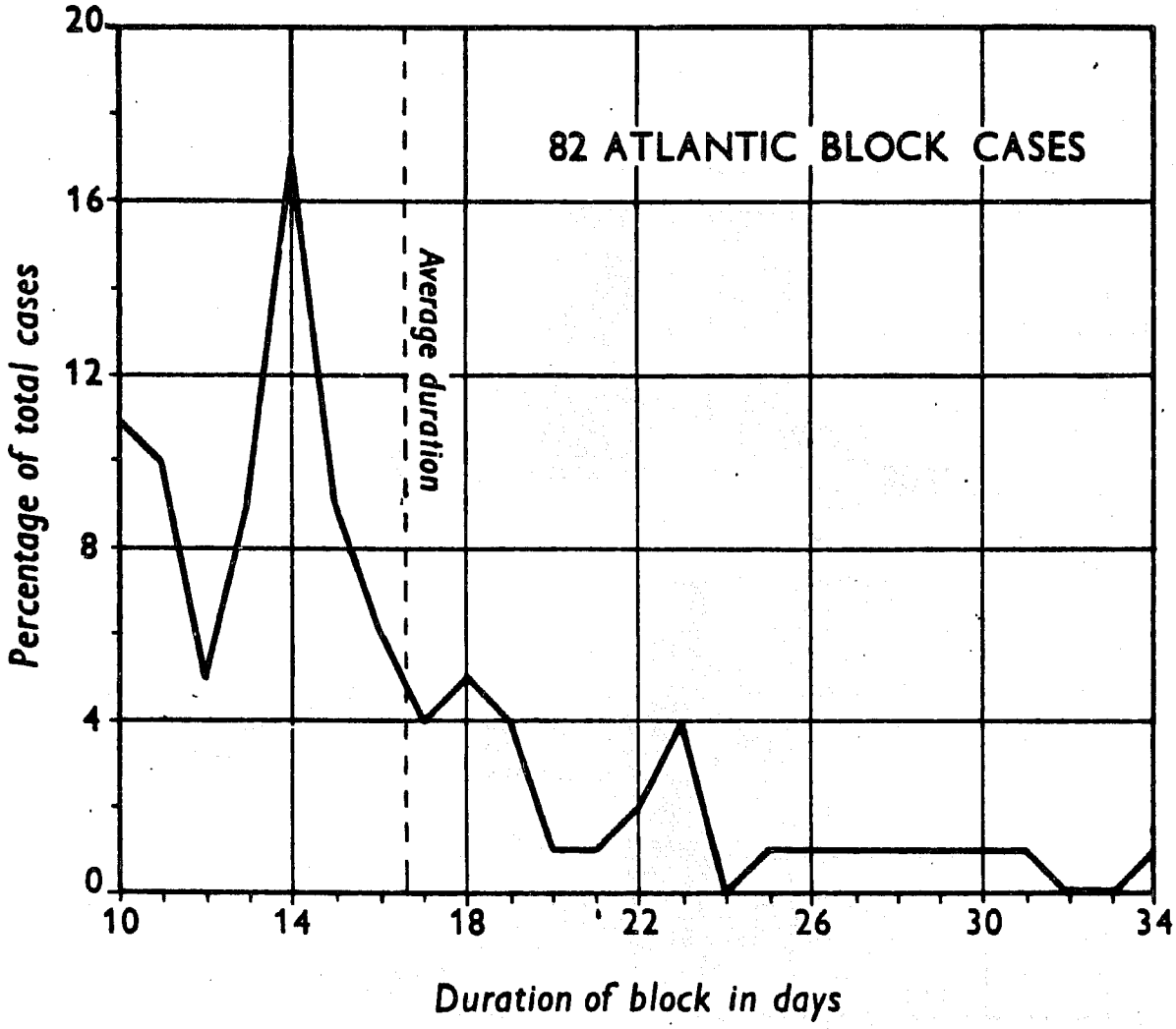

Fig. 2.3 Persistence of blocking action in the Atlantic area; the straight-line frequency graph shows the distribution by duration of 82 cases of Atlantic block development. Cases (4%) with periods longer than 34 days are not shown in the figure (from Rex, Tellus, 1950).

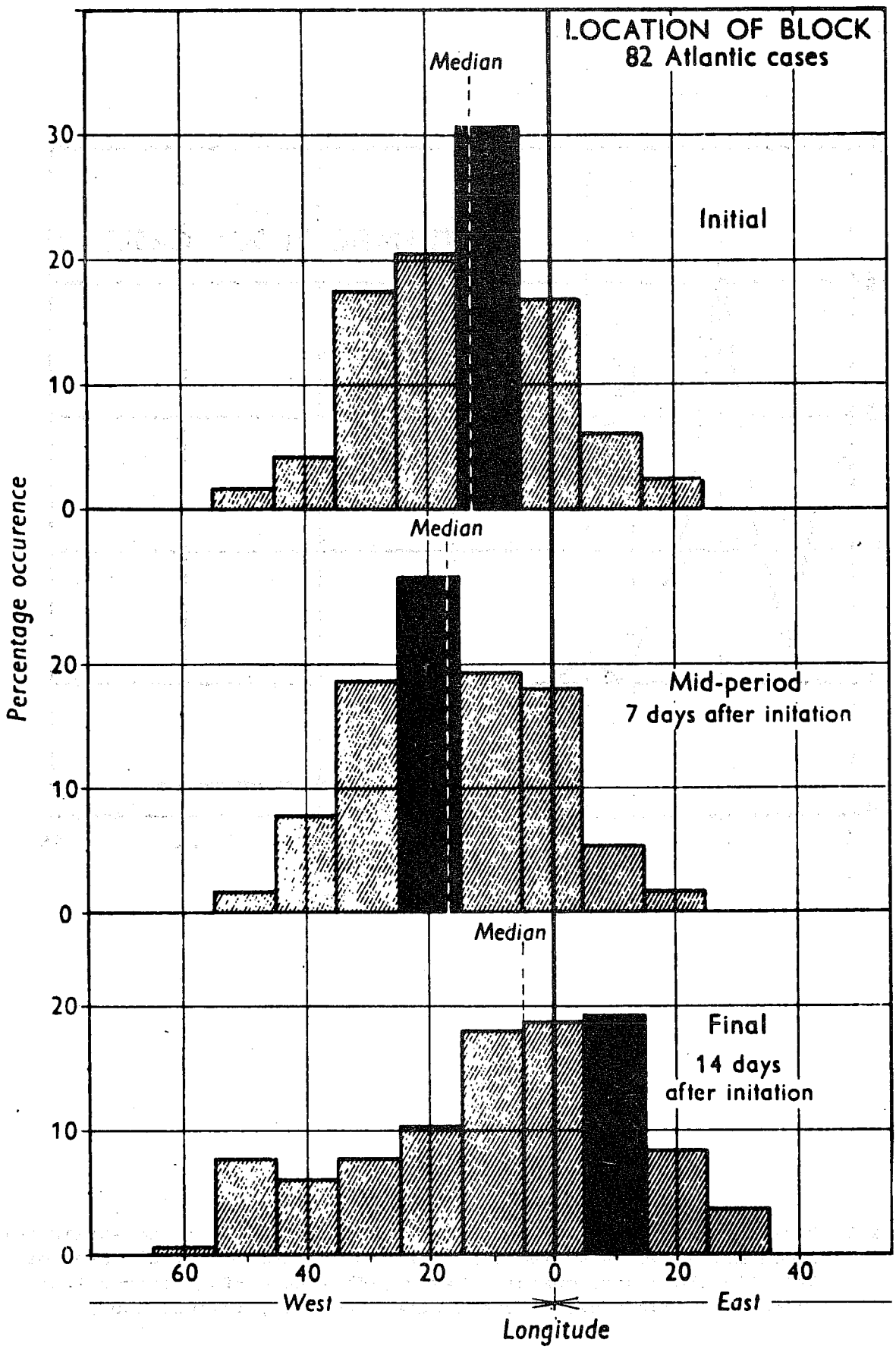

Fig. 2.4 Movement characteristics of Atlantic blocks; the series of histograms shows the frequency distribution in longitude of 82 cases of Atlantic block development - initially, at mid-period and finally (just prior to dissipation). Modes shaded black. Positions were determined at mid-tropospheric level (from Rex, Tellus, 1950).

3. BLOCKING PATTERN AND ENERGY DISPERSION

Several theories have been suggested to explain the blocking phenomenon. A good theory ought to describe the most dominating features of the blocking highs, i.e., the splitting of the jet upstream of the high, the persistence of the pattern, the preference for certain localities and the strong seasonal dependence.

Numerical experiments with a barotropic model including topographical forcing have produced quasi-equilibrium phenomena, reminding very much of blocking, Egger (1978). Although the actual atmosphere naturally is baroclinic it is very likely the blocking, due to its scale, must have a counterpart in a simple barotropic atmosphere and the baroclinic forcing may be regarded as a secondary effect and only act as additional forcing on the planetary scale motion. The theories for blocking which we will describe in this lecture will be restricted to the barotropic model.

We will make use of the barotropic equation in the following form

$$\frac{d}{dt}\left(\frac{f+\zeta}{D}\right) = 0 \tag{3.1}$$

where D is the depth of the atmosphere, ζ the relative vorticity, and f the Coriolis parameter. Assuming the north-south motion to be geostrophic and the perturbation to be small, the vorticity equation can be written in the following form on a β-plane:

$$\frac{\partial^3 D'}{\partial x^2 \partial t} + U\frac{\partial^3 D'}{\partial x^3} + \beta\frac{\partial D'}{\partial x} - \lambda^2\frac{\partial D'}{\partial t} = 0 \tag{3.2}$$

where $\lambda^2 \equiv \frac{f^2}{gD_o}$, D_o is the undisturbed depth, and D' the perturbation of the free surface; $D = D_o + D'$.

The phase speed, c, of the perturbation is

$$c = \frac{4\pi^2 U - \beta L^2}{4\pi^2 + \lambda^2 L^2} \tag{3.3}$$

where U is the zonal mean wind speed, L the wavelength and

$$\beta = \frac{\partial f}{\partial y}$$

The energy is propagated by the group velocity, which because of the dispersive character of the flow, is different from that of the prevailing current. The group velocity, c_g, is defined

$$c_g = \frac{\partial \nu}{\partial k} = c - L \frac{\partial c}{\partial L} \tag{3.4}$$

where ν is the frequency and k is the wavenumber.

The corresponding group velocity to equation (3.3) takes the form

$$c_g = \frac{4\pi^2 U + \beta L^2 + 2\lambda^2 L^2 c}{4\pi^2 + \lambda^2 L^2} \tag{3.5}$$

As can be seen from (3.5) the group velocity can be negative and energy be propagated upstream. This is not the case when $\lambda = 0$ and consequently we need to consider a free surface if we should be able to describe upstream propagation of wave-energy, Fig. 3.1. In the following we will investigate the dispersive properties of a solitary wave described by Yeh (1949). We will show how the dispersion of the solitary wave very strongly depends on the latitude and that the behaviour bears resemblance to a blocking wave once the block has been established. The incorporation of a free surface is necessary in order to describe the characteristic feature of the blocking pattern to have a gradual westward progression. Following Yeh we will write

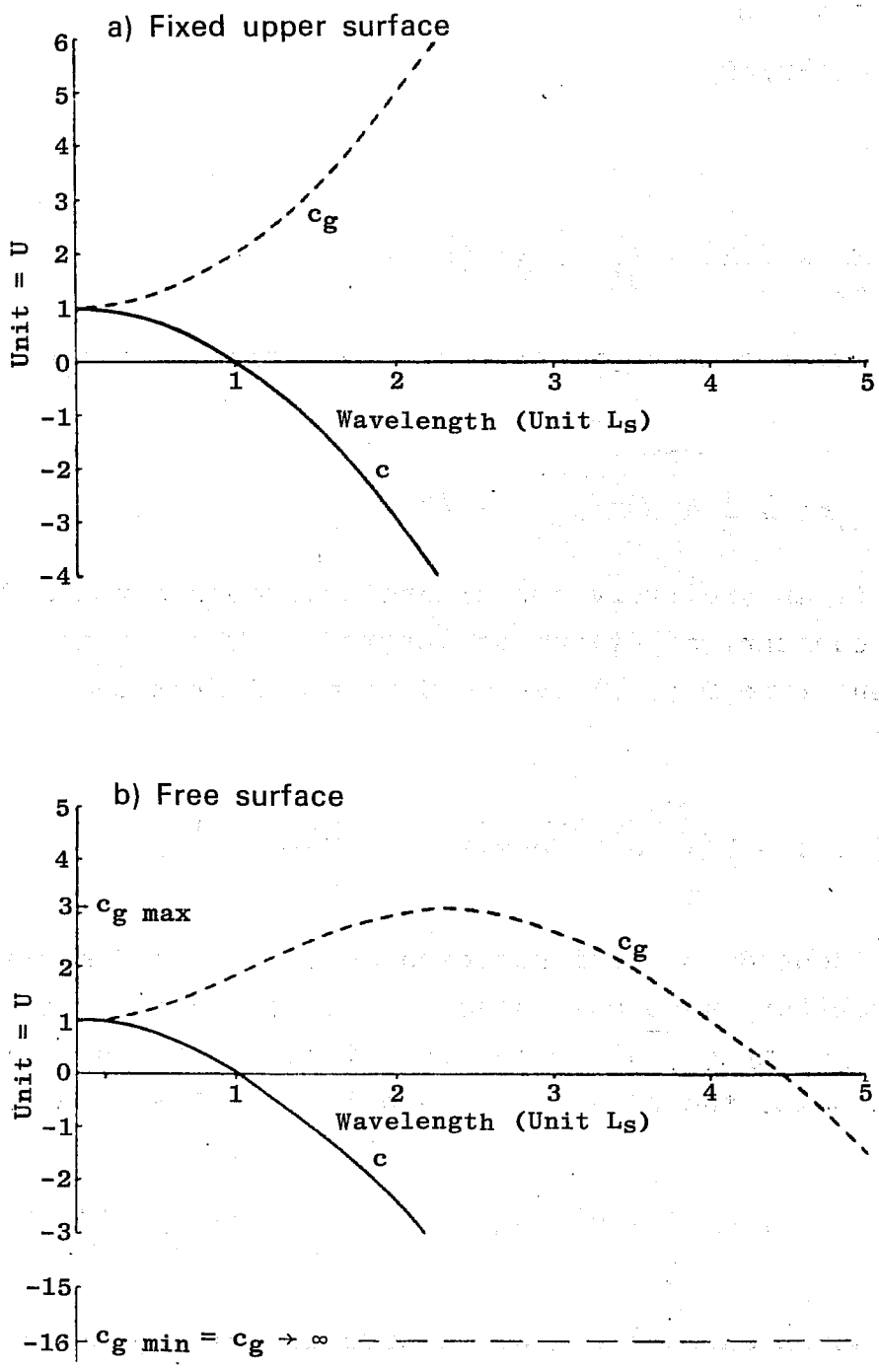

Fig. 3.1 (a) Group velocity (broken line) and phase velocity (solid line) as a function of wave length for a fixed upper surface.
(b) Group velocity (broken line) and phase velocity (solid line) as a function of wave length for a free upper surface. Both curves are limited by the horizontal asymptotic line $c_g=c_g$ (min) (from Yeh, J. of Met. 1949).

equation (3.2) in a non-dimensional form using the scaling parameters

$$\xi = kx$$

$$\tau = t\sqrt{\beta U}$$

$$A^2 = f^2U/gD_o\beta$$

which gives

$$\frac{\partial^3 D'}{\partial \xi^2 \partial \tau} + \frac{\partial^3 D'}{\partial \xi^3} + \frac{\partial D'}{\partial \xi} - A^2 \frac{\partial D'}{\partial \tau} = 0 \qquad (3.6)$$

Let us next assume an initial solitary wave be represented by

$$D'(\xi,0) = \frac{1}{2} B \sqrt{\pi}\, a^{-1} e^{-\xi^2/a^2} \qquad (3.7)$$

where a is an arbitrary non-dimensional constant and B another constant of dimension length. Then at any subsequent time $D'(\xi,\tau)$ can be determined from the following integral

$$D'(\xi,\tau) = B \int_0^\infty e^{-a^2k^2} \cos\left(k\xi - \tau \frac{k^2 - k}{A^2 + k^2}\right) dk \qquad (3.8)$$

Since A^2 depends on latitude(because of β) the dispersion of the solitary wave must also be a function of latitude. If we for example could maintain a final zonal current U near the pole, the $A^2 \to \infty$ at the pole and (3.8) becomes

$$D'(\xi,\tau) = B \int_0^\infty e^{-a^2k^2} \cos\, k\xi dk = \frac{1}{2} Ba^{-1}\sqrt{\pi}\, e^{-\xi^2/4a^2}$$

This equation shows that once a pressure rise or fall is formed near the pole it would remain there without being dispersed. This would correspond to an extremely slowly moving blocking wave.

a) Equator

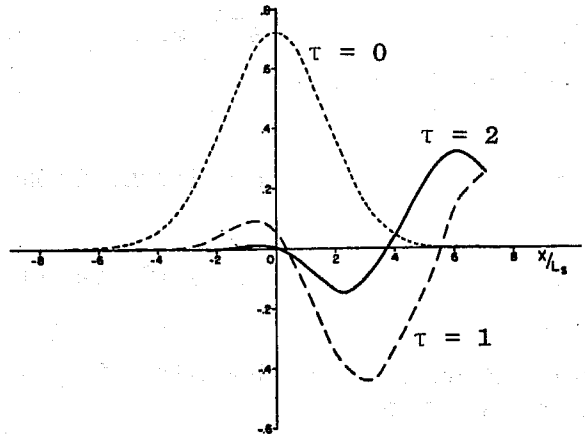

b) 40° Latitude

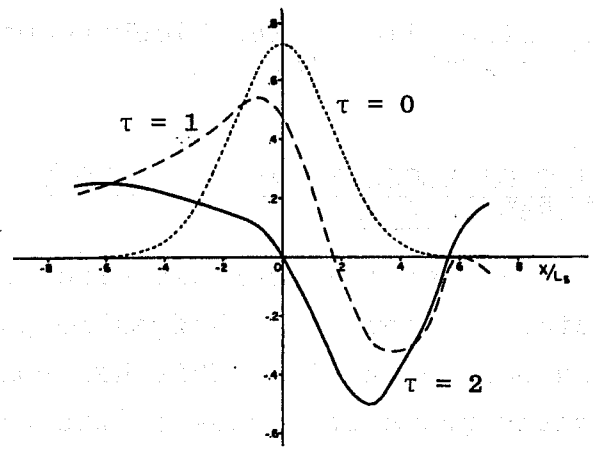

c) 70° Latitude

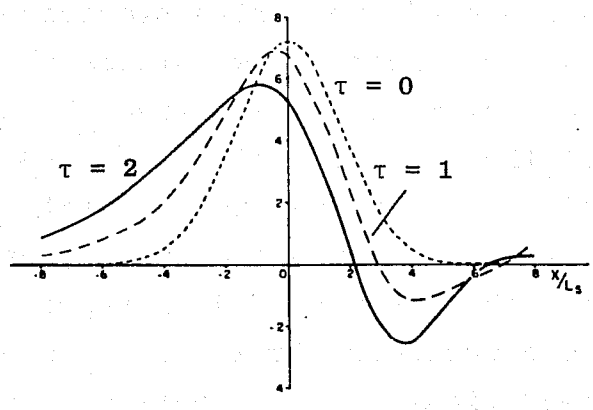

Fig. 3.2 Dispersion of an initial solitary wave at 3 different latitudes. The time unit, τ, is approximately 1 day and the space unit, ξ, on the horizontal axis is 1000 km. (a) at the equator, (b) at 40^{o} latitude and (c) at 70^{o} latitude (from Yeh, J. of Met. 1949).

Fig. 3.2 shows a numerical evaluation of (3.8) for three different latitudes. $U = 17\ ms^{-1}$ and $D_o = 8.10\ m^3$ have been used as numerical values.

The following conclusions can be drawn from Yeh's study

(i) Blocking effect is a high latitude phenomenon

(ii) The intensity of the blocking wave increases with latitude

(iii) The speed of the blocking wave decreases with latitude

(iv) The life time of the blocking wave increases with latitude.

4. DEVELOPMENT OF BLOCKING AS AN ANALOGY TO THE HYDRAULIC JUMP

Rossby (1950) suggested that certain kinds of blocking at least superficially resembled a hydraulic jump of a type which occurs in open channels. This happens when the speed of the water grows in excess of the critical value $\sqrt{gD}$, where D is the depth of the water and g is the acceleration of gravity. The development of stationary hydraulic jumps in streams and channels is made possible by the fact that under steady state conditions with prescribed values for volume and momentum transport two states of motion are possible, one of which is characterised by the water speed, u, in excess of the critical value, $\sqrt{gD}$, and another speed below the critical value. The former state of motion is accompanied by a higher rate of energy transfer downstream than the latter. The hydraulic jump represents a sudden transition from a super-critical flow at a high energy level to a sub-critical state of motion at a lower energy level. In the jump itself a fraction of the kinetic energy of the basic flow is transformed into eddy energy.

Following Rossby we shall consider a horizontal westerly jet in a non-divergent incompressible atmosphere. We will show that for a constant volume transport the momentum transfer across a vertical plane normal to such a jet possesses a minimum value. Hence if the flow is at all possible dynamically, two solutions exist which are compatible with the continuity and momentum requirements. Since these solutions represent different energy levels a necessary requirement for the development of jumps is thus fulfilled.

Consider a jet with the speed $u = \dot{x}$, x pointing eastward and independent of y (pointing northward) the pressure distribution can be computed from

$$\frac{\partial p}{\partial y} = - \rho f u \tag{4.1}$$

where ρ is the density and f the Coriolis parameter. If p_N and p_S represent the undisturbed pressures to the north and south (Fig. 4.1) it follows that

$$p_S - p_N = \rho \int_{-a}^{+a} f u \, dy \tag{4.2}$$

where we have extended the integration across the entire current width 2a with the origin of the coordinate system in the centre of the jet. A constant value of f gives

$$p_S - p_N = \rho f V \quad \text{where } V = 2au \tag{4.3}$$

represents the volume transport. It is evident that a uniform slowing down of the current, followed by a compensating broadening of its width, will leave the pressure on individual fluid filaments unchanged (see dashed lines across the channel in Fig. 4.1). Thus in this dynamical model there would be no way of reducing the speed of the current in the manner observed in a typical blocking wave.

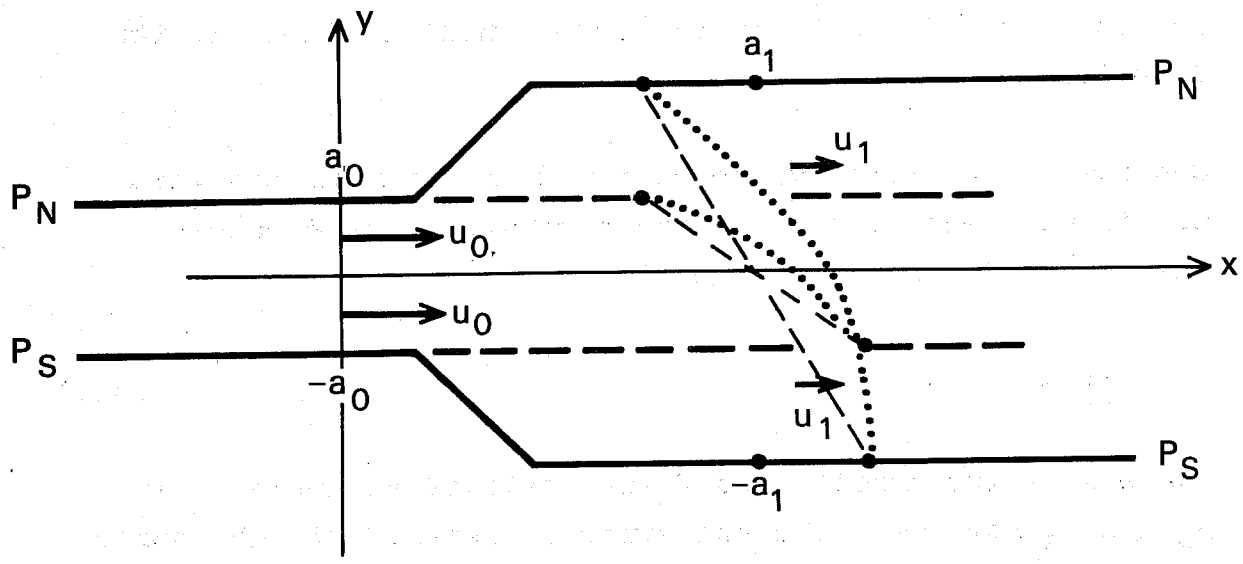

Fig. 4.1 Jet flow in a channel bounded by 2 pressure surfaces P_N and P_S. The thin dashed lines show the pressure profiles for the narrow as well as for the wide part of the channel when f is constant. The dotted lines show the pressure profiles respectively when the β-effect is incorporated. For further information see text.

If one on the other hand allows for the fact that the Coriolis parameter depends on latitude by setting

$$f = f_o + \beta y \tag{4.4}$$

the pressure distribution may be computed from

$$p = p_S - \rho f_o \int_{-a}^{y} u \, dy - \rho\beta \int_{-a}^{y} y \, u \, dy \tag{4.5}$$

This pressure distribution is given by the dotted line in Fig. 4.1. If $\bar{p}$ is the pressure distribution corresponding to the case of constant f and p' the additional pressure field associated with β, so that

$$p = \bar{p} + p'$$

it follows that

$$p' = -\rho\beta \int_{-a}^{y} y \, u \, dy = \rho\beta \frac{a^2 - y^2}{2} u \qquad (y^2 < a^2) \tag{4.6}$$

It is easily seen that this pressure excess (difference between the dashed and dotted line in Fig. 4.1) vanishes in the undisturbed atmosphere surrounding the jet and reaches its maximum in the centre where

$$p'_{max} = \rho\beta u \frac{a^2}{2} \tag{4.7}$$

For a constant transport (V = 2 au) it follows that

$$p'_{max} = \rho\beta V \frac{a}{4} \tag{4.8}$$

Thus the pressure excess increases with increasing width (or increasing speed) of the jet and it follows that a possibility exists for the setting up of an internal mechanism through which the speed of the current may be reduced.

Some numerical values (MTS-units) give:

$\beta = 2.10^{-11}$, $a = 10^6$ m, $u = 40$ ms^{-1}, $\rho = 10^{-3}$ $\rightarrow$ $p'_{max} = 4$ mb

$\beta = 2.10^{-11}$, $a = 2.10^6$ m, $u = 20$ ms^{-1}, $\rho = 10^{-3}$ $\rightarrow$ $p'_{max} = 8$ mb

The momentum transfer, MOT, in the jet can be calculated as follows

$$\rho \frac{du}{dt} = \rho f v - \frac{\partial p}{\partial x} \tag{4.9}$$

or

$$\rho \frac{du}{dt} - \rho f \frac{dy}{dt} + \frac{\partial p}{\partial x} = 0$$

or since

$$\frac{df}{dt} = \beta v = \beta \frac{dy}{dt}$$

we obtain

$$\rho \frac{d}{dt} (u - fy + \frac{\beta y^2}{2}) + \frac{\partial p}{\partial x} = 0 \tag{4.10}$$

Integration between fixed walls assuming steady states gives

$$MOT = \int_{-a}^{a} u \, (u + \frac{\beta y^2}{2}) dy = \text{constant} \tag{4.11}$$

We have also here made use of the fact that $\frac{\partial p}{\partial x} = 0$ to the north and the south of the jet and that $\frac{dv}{dt}$ vanishes in the region of parallel flow outside the blocking zone.

We shall apply the result of equation (4.11) to a simple barotropic current of constant speed u and width 2a. If the corresponding quantities upstream from the jump are indicated by u_o and $2a_o$ it follows that the momentum transfer (MOT) apart from a factor ρ, is given by:

$$MOT = 2au^2 + \frac{\beta u a^3}{3} = 2 a_o u_o^2 + \frac{\beta u_o a_o^3}{3} \tag{4.12}$$

The volume transport V is given by

$$V = 2au = 2a_o u_o \tag{4.13}$$

The momentum transfer can now be written

$$MOT = V(u + \frac{\beta V^2}{24u^2}) \tag{4.14}$$

MOT expressed by equation (4.14) reaches a minimum when $u^3 = \frac{\beta V^2}{12}$. In Fig. 4.2 we have illustrated the case where the channel width is $a = 10^6$ m and where the initial windspeed is $u_o = 30$ ms^{-1}. We can see that there are 2 permissible states having the same MOT for the windspeeds 30 ms^{-1} and 11.8 ms^{-1}. It follows further that there are always two permissible modes when $u_o > u_{oo} = \beta \frac{a^2}{3}$ which we will call the critical velocity. For an initial channel width of $a_o = 10^6$m, $u_{oo} = 7$ ms^{-1} and for a channel width of $a_o = 2.10^6$, $u_{oo} = 28$ ms^{-1}.

It is suggested that a current with a super-critical value of u can break down into a flow with a lower energy level. It is further suggested that this break down takes the form of two branches of the original jet with a pressure rise or a block ($p' > 0$) in the middle between the two jet branches.

5. BLOCKING AND LARGE SCALE FORCING

The idea proposed by Rossby that the hydraulic jump could explain the mechanism of blocking received some criticism during the years. The development of blocking is by no means a rapid process and there is in fact no observational evidence for the possible violent eddy motion which one could expect in association with an hydraulic jump.

The fact that the blocking is mainly a phenomenon in the Northern Hemisphere, at least in its most developed form, and also due to the fact that it is observed in certain areas only, suggests that forcing processes are of major importance.

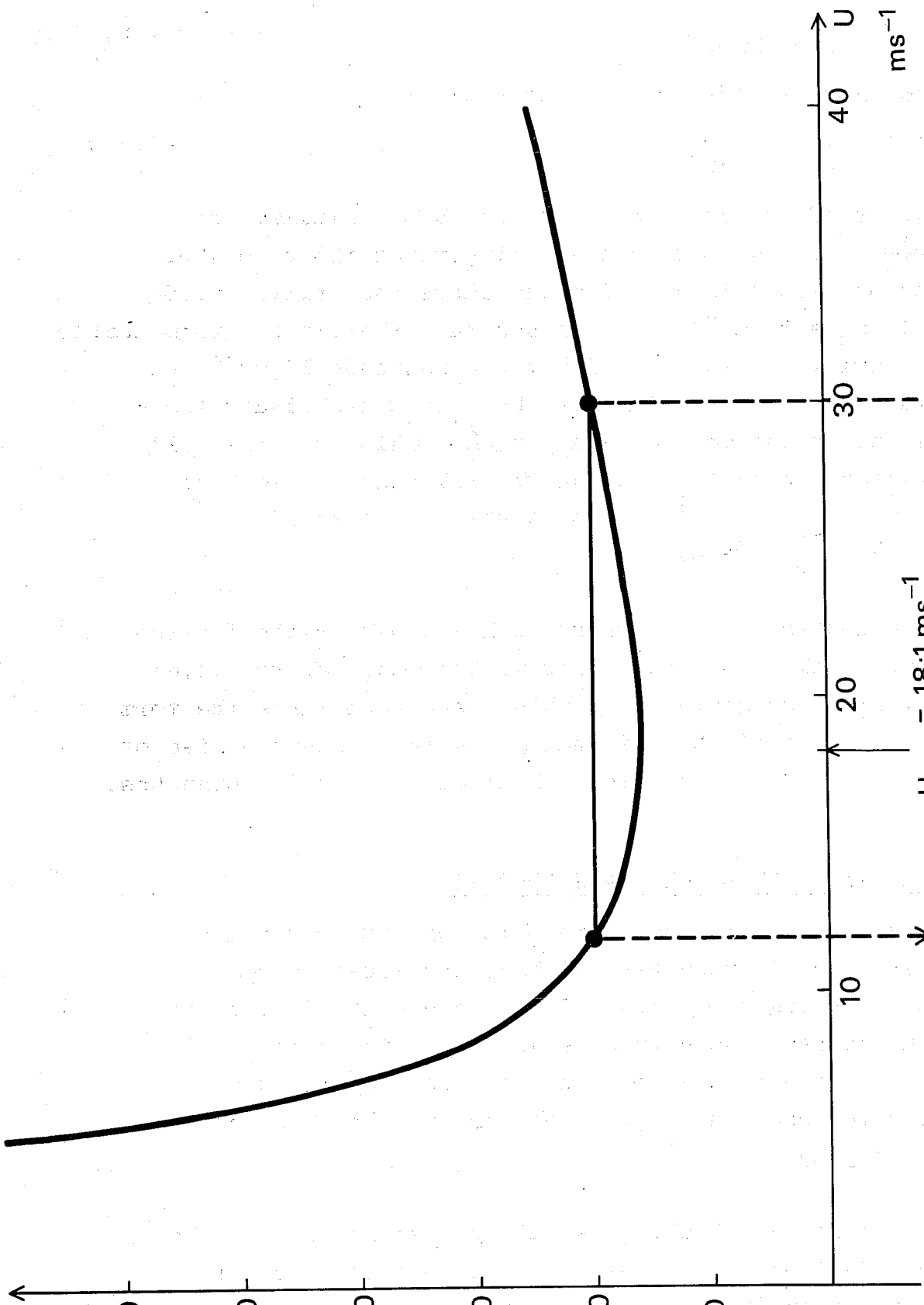

Fig. 4.2 MOT (momentum transfer) as a function of u according to eq.4.14. An initial windspeed u_o = 30ms^{-1} gives 2 permissible states indicated by vertical dashed lines in the figure. Units MTS. For further information see text.

Fig. 5.1 shows the flow pattern which develops in a barotropic atmosphere when integrated over a sphere. The flow is obtained after a 10 day integration using a barotropic version of the ECMWF grid point model. The integrations have started from a zonal flow (January climatology at 500 mb). A smooth topography has been used identical to what is used in the ECMWF operational model. It is indicated that there are 2 regions where the flow is weakened; namely around 40W to 10W and 170W to 130W. These are the areas where blocking is mainly observed. Two intense jets can be seen over the east coast of Japan and the east coast of the United States of America. Clearly, baroclinic developments in these regions will further intensify the two ridges downstream through the action of dispersion processes. Namias (1964) stresses the idea that the physical causes of the blocks lie in a feedback mechanism between the atmosphere and the surface.

Egger (1978) recently carried out some simple numerical experiments using a highly truncated version of the barotropic vorticity equation with Newtonian forcing. The flow patterns in Fig. 5.2 suggest that non-linear interaction between a forced wave and the ultra long planetary waves produce patterns which are very similar to blocking patterns.

We will next turn our attention to a paper by Charney and DeVore (1979). An investigation by a low-order barotropic model in a β-plane channel with forcing can be shown to have a multiplicity of stationary or oscillating states, each presumably with its own class of smaller scale instabilities and each state presumably capable of undergoing transitions with the aid of these instabilities from one state to the other.

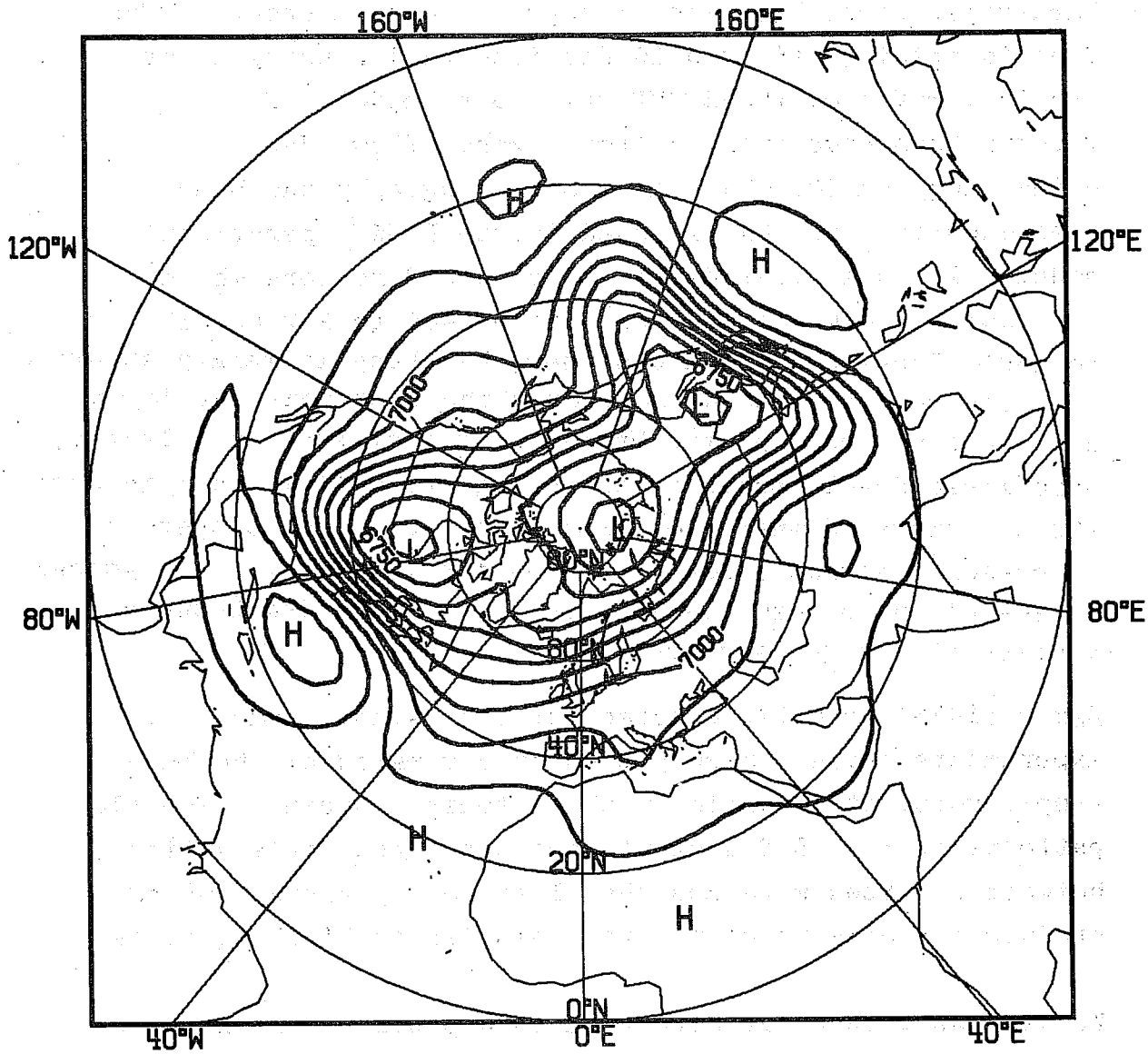

Fig. 5.1 Flow pattern at a free barotropic surface and forced by the earth topography. The flow is the result of a 10-day global grid point integration starting from a zonal climatological flow at 500 mb. (By courtesy of J. Quiby).

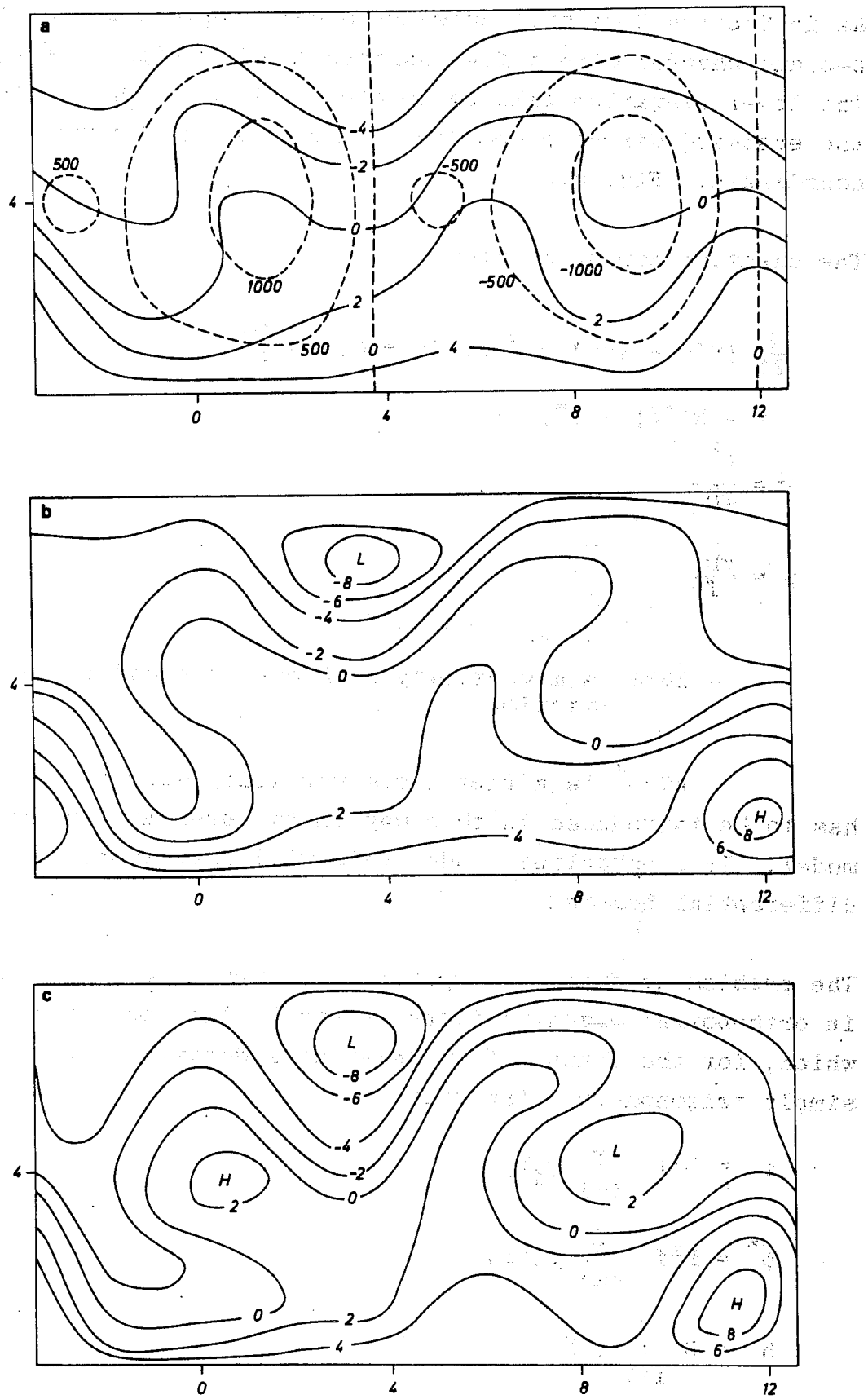

Fig. 5.2 Blocking in a channel caused by Newtonian forcing. Streamfunction ψ ($10^7 m^2 s^{-1}$) at day 10 (a), 20 (b) and 25 (c). Isopleths of the orography (m) are dashed. From Egger, J.Atmos. Sci.,(1978).

As in Section 3 we will consider a barotropic model on a β-plane channel with a free surface of the height $D = D_o + D'$. The lower elevation will be denoted by $h(x,y)$ where x is the the eastward directed coordinate and y the northward directed coordinate. Fig. 5.3.

The equation can be written

$$\frac{\partial}{\partial t}(\nabla^2\psi - \lambda^2\psi) + J(\psi, \nabla^2\psi + h) + \beta\frac{\partial\psi}{\partial x} \qquad (5.1)$$

$$= -k\nabla^2(\psi - \psi^*)$$

$$\lambda^2 = \frac{f^2}{gD_o}$$

$$\psi = \frac{gD'}{f}$$

$-k\nabla^2\psi$ is a vorticity sink due to boundary layer friction

$k\nabla^2\psi^*$ is a ficticious vorticity source term which has to be introduced in this way in the present barotropic model. In a baroclinic model this will correspond to differential heating.

The problem is further simplified by expanding ψ, ψ^* and h in orthonormal eigenfunctions of the Laplace operator, which, for the channel flow under consideration, are simply trigonometric functions,

$$\psi = L^2 f \sum_{i=1}^{\infty} \psi_i F_i$$

$$\psi^* = L^2 f \sum_{i=1}^{\infty} \psi_i^* F_i \qquad (5.2)$$

$$h = D \sum_{i=1}^{\infty} h_i F_i$$

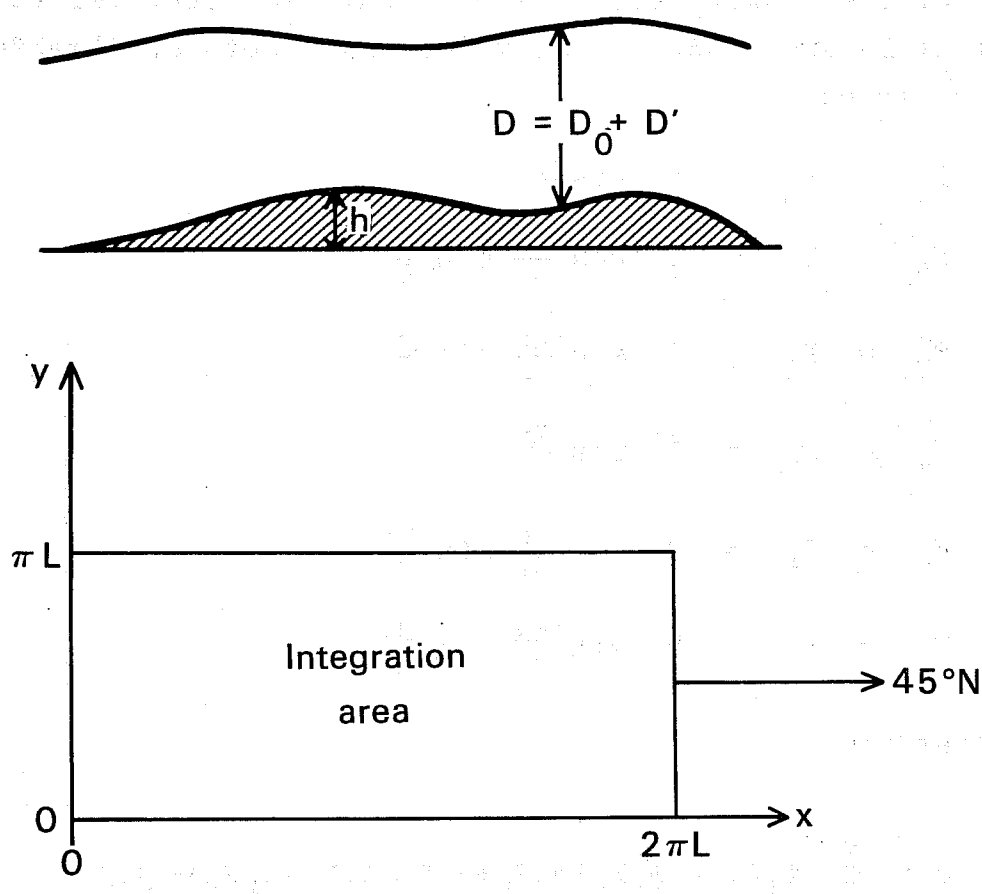

Fig. 5.3 Upper part of figure illustrates a barotropic channel with a free surface and with the height D. The orography with the height, h is dashed. Lower part of figure shows the integration area. For further information see text.

where

$$L^2\nabla^2 F_i = - a_i^2 F_i \tag{5.3}$$

and

$$\frac{\partial F_i}{\partial x} = 0 \text{ at } y = 0, \pi L \tag{5.4}$$

are used in order to satisfy the condition of no normal flow at the boundaries. The procedure is identical to that of Lorenz (1963). The following 6 sets of eigenfunctions are selected :

$$\begin{aligned}
F_1 &= F_A = \sqrt{2} \cos \frac{y}{L} \\
F_2 &= F_K = 2 \cos \frac{nx}{L} \sin \frac{y}{L} \\
F_3 &= F_L = 2 \sin \frac{nx}{L} \sin \frac{y}{L} \\
F_4 &= F_C = \sqrt{2} \cos \frac{2y}{L} \\
F_5 &= F_M = 2 \cos \frac{nx}{L} \sin \frac{2y}{L} \\
F_6 &= F_N = 2 \sin \frac{nx}{L} \sin \frac{2y}{L}
\end{aligned} \tag{5.5}$$

and setting

$$\psi = \sum_{i=1}^{6} \psi_i F_i = \psi_A F_A + \psi_K F_K + \psi_L F_L + \psi_C F_C + \psi_M F_M + \psi_N F_N \tag{5.6}$$

and similar expressions for ψ^* and h.

The first orthogonal function, F_A, permits a zonal flow component which varies from zero at the boundaries to a maximum at the centre of the channel; the fourth, F_C, permits a zonal flow component with both a maximum and a minimum in the interior.

The y-amplitudes of the corresponding pairs of wave functions (F_K, F_N) have, respectively, one and two maxima in the interior. If F_j and F_k are two arbitrary eigenfunctions, then owing to their orthonormal property

$$L^2 J(F_j,F_k) = \sum_{j=1}^{\infty} c_{ijk} F_i \ , \tag{5.7}$$

where

$$c_{ijk} = L^2 \overline{F_i J(F_j,F_k)} \tag{5.8}$$

with the bar operator denoting a horizontal average. It follows by definition that $c_{ijk} = - c_{ikj}$ and from the boundary condition that $c_{ijk} = c_{jki} = c_{kij}$.

We also have

$$\frac{\partial F_i}{\partial x} = \sum_{j=1}^{\infty} b_{ij} F_j \ , \ b_{ij} = F_i \overline{\frac{\partial F_i}{\partial x}} \tag{5.9}$$

Non-dimensionalising

$$\dot{\psi}_i = (a_i^2+\lambda^2)^{-1} \left\{ \sum_{k>j}^{\infty} c_{ijk} \cdot \left\{(a_j^2-a_k^2)\psi_j \ \psi_k - h_j\psi_k + h_k\psi_j\right\} + \beta \sum_{j=1}^{\infty} b_{ji} \psi_j - ka_i^2(\psi_i-\psi_i^*)\right\} \tag{5.10}$$

For simplicity and to ensure that we are dealing with large topographic scales only the first topographic wave mode K will be considered and we have for the non-dimensionalised, h

$$h = \frac{h_o}{2D} F_K$$

We will next introduce zonal driving and dissipation in the first y-mode by fixing ψ_A^* and setting the other spectral components of ψ^* equal to zero. It can be seen from equation (5.10) that if the second y-mode components are zero initially, they will remain zero. The system will be governed by

$$\dot{\psi}_A = - k(\psi_A - \psi_A^*) + h_{o1} \psi_L \tag{5.11}$$

$$\dot{\psi}_k = - k \psi_k - b_{n1} \psi_L \tag{5.12}$$

$$\dot{\psi}_L = - k \psi_L + b_{n1} \psi_k - h_{n1} \psi_A \tag{5.13}$$

Here

$$h_{o1} = \frac{8\sqrt{2}}{3\pi} (1 + \lambda^2)^{-1} \frac{h_o}{2D}$$

$$b_{n1} = \frac{40\sqrt{2}}{15\pi} \frac{n}{n^2 + 1} \psi_A - \frac{L}{a} \frac{n}{n^2 + 1} \tag{5.14}$$

$$h_{n1} = \frac{8\sqrt{2}}{3\pi} n(n^2 + 1 + \lambda^2)^{-1} \frac{h_o}{2D}$$

Here a is the radius of the earth.

At equilibrium these equations yield

$$\frac{\psi_L}{h_{n1}} = \frac{k}{h_{o1} h_{n1}} (\psi_A - \psi_A^*) \tag{5.15}$$

$$\frac{\psi_L}{h_{n1}} = - \frac{k}{b_{n1}^2 + k^2} \psi_A \tag{5.16}$$

$$\frac{\psi_k}{h_{n1}} = \frac{b_{n1}}{b_{n1}^2 + k^2} \psi_A \tag{5.17}$$

from which ψ_A, ψ_k and ψ_L can be found by equating (5.15) and (5.16) and solving the resulting cubic equation in ψ_A. It is found that for a large range of parameter values there are three separate equilibrium values of ψ_A. By calculating the characteristic equation to the equations (5.11 to 5.13) it is found that when there is only one equilibrium this is always stable. In the case of three equilibriums the intermediate value of ψ_A is unstable, while the other 2 remain stable for first mode perturbations. However, the one with the small value of ψ_A become unstable for second mode perturbation when the zonal driving ψ_A^* is sufficiently large. There is consequently a range of values for which 2 stable equilibria exist. The unstable equilibrium being found, cannot be barotropic instability of the zonal flow, since $\beta - U_{yy}$ does not vanish. This instability is therefore solely due to the interaction of the topographic wave with the zonal mean flow.

Fig. 5.4 shows the transition from an unstable equilibrium towards a low index stable equilibrium. In this case a point in the first mode phase space, close to the unstable fixed point, finds itself in the attractor basin of one or the other of two stable fixed points and winds down into one of them. However, when one of the stable fixed points becomes unstable for mixed mode perturbations its representative point in the extended phase space need not find itself in the attractor basin of the other stable fixed point and the system may oscillate. This oscillation can occur even if the mountain amplitude goes to zero. Fig. 5.5 examplifies such a state.

In order to confirm these spectral low order integrations, numerical integrations were carried out on a 16 x 16 grid point model using the same geometry, dissipation and forcing as in the spectral model and with initial conditions taken as equilibrium solutions of the truncated spectral model. Fig. 5.4b and Fig. 5.5c and 5.5d confirm very well

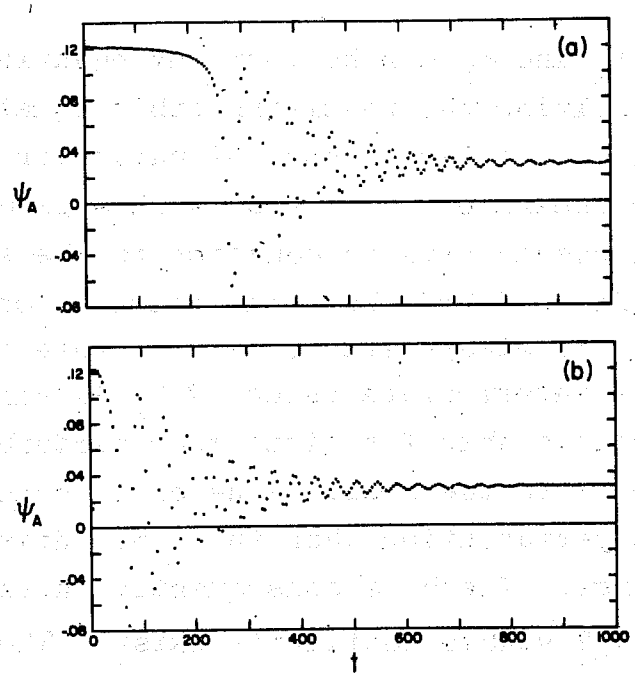

Fig. 5.4 Transition from an unstable, first mode, middle-index state to a stable, first mode, low index state. (a) spectral model, (b) grid point model. From Charney and DeVore, J.Atmos.Sci., (1979).

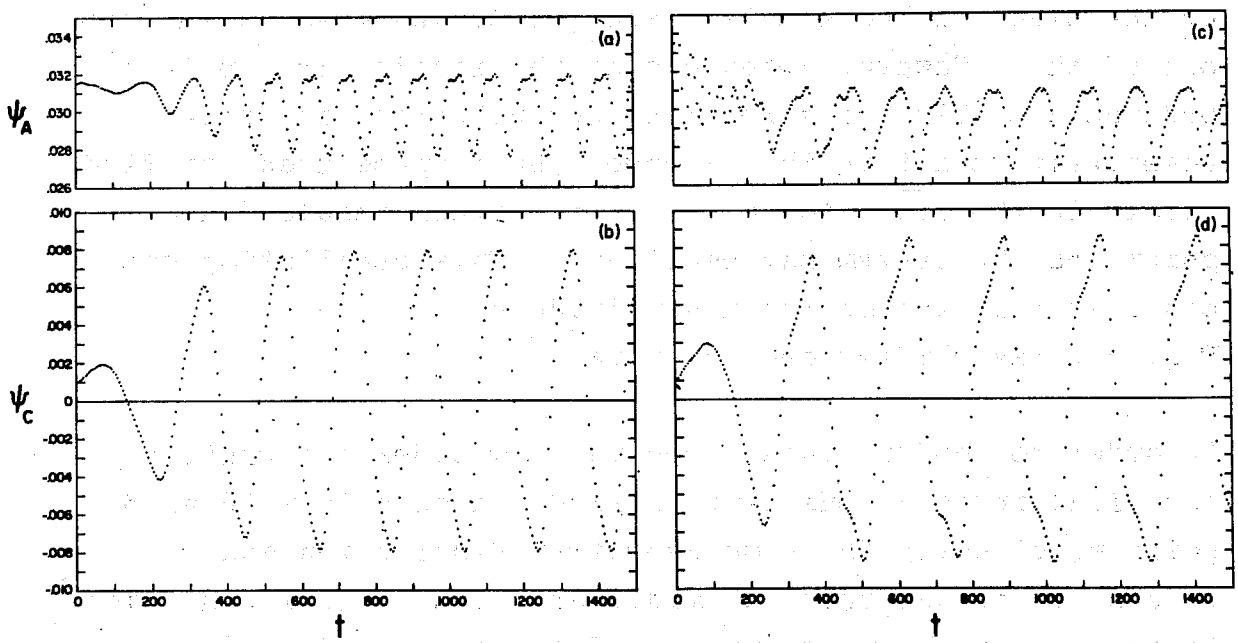

Fig. 5.5 Oscillation of a topographically forced flow. (a) and (b) are the first and second mode zonal streamfunction amplitudes as a function of time for the truncated spectral model; (c) and (d) are for the grid point model. From Charney and DeVore. J. Atmos.Sci., (1979).

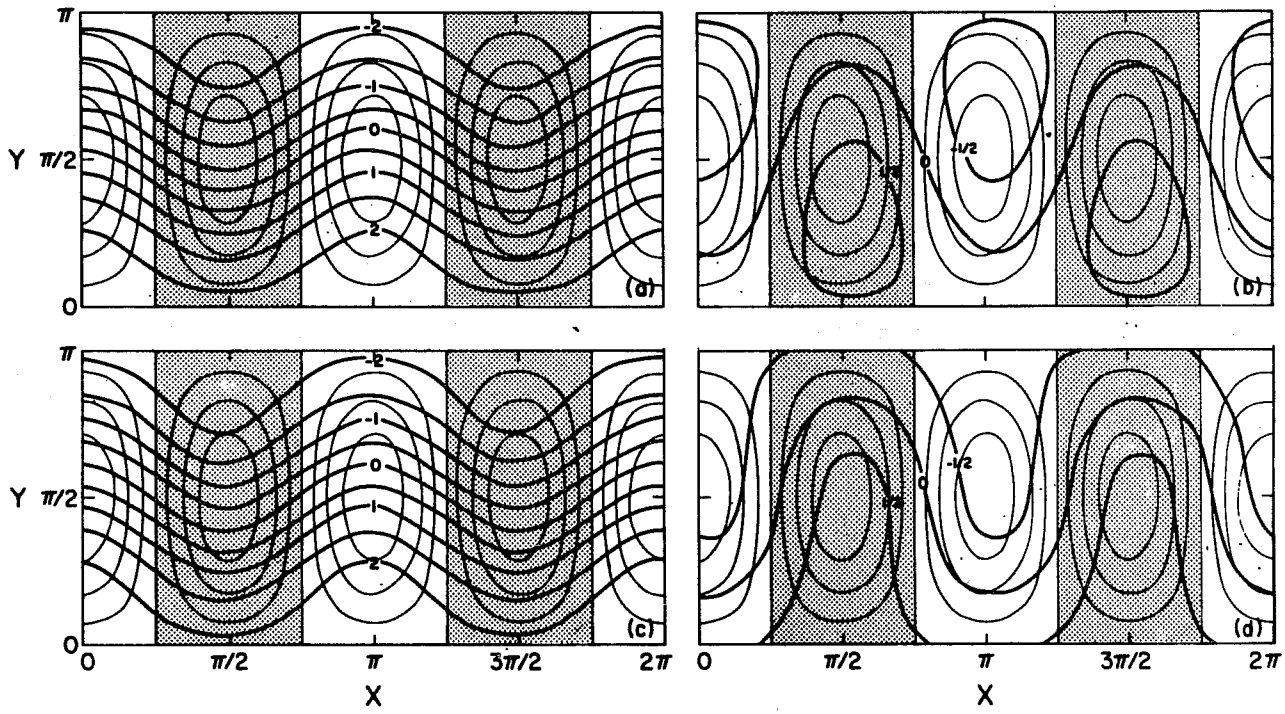

Fig. 5.6 Streamfunction fields of the stable first mode equilibria of a topographically forced flow. (a) and (b) for the spectral model; (c) and (d) for the grid point model. From Charney and DeVore, J. Atmos. Sci., (1979).

the results with the low order system. Fig. 5.6 gives the corresponding streamfunction field for the two stable regimes and for the spectral and grid point model respectively. It is interesting to note the similarity to a low index and a high index circulation in the atmosphere.

References

Berggren, R., Bolin, B., and Rossby, C. G., 1949: An aerological study of zonal motion, its perturbation and break down. Tellus, 1, 14-37.

Charney, J., and DeVore, J. 1979: Multiple flow equilibria in the atmosphere and blocking. J.Atmos.Sci., 36, 1205-1216.

Egger, J., 1978: Dynamics of blocking high. J.Atmos.Sci., 35, 1788-1801.

Garrott, E.B., 1904: Long range forecasts. U.S. Weather Bureau Bulletin, No. 35.

Lorenz, E.N., 1963: The mechanics of vacillations. J.Atmos.Sci., 20, 448-464.

Namias, J., 1964: Seasonal persistence and recurrence of European blocking during 1958 - 1960. Tellus, 16, 394-407.

Rex, D.F., 1950a: Blocking action in the middle troposphere and its effect upon regional climate. I. An aerological study of blocking action. Tellus, 2, 196-211.

Rex, D.F., 1950b: II. The climatology of blocking action. Tellus, 2, 275-301.

Rossby, C.G., 1950: On the dynamics of certain types of blocking waves. J.Chin.Geophys.Soc., 2, 1-13.

Taljaard, J. J., 1972: Synoptic Meteorology of the Southern Hemisphere, see p.182-189 in Meteorology of the Southern Hemisphere. A.M.S. Meteorological Monographs, Volume 13, Number 35, Ed. C. Newton.

Yeh, T.C., 1949: On energy dispersion in the atmosphere. J.Meteor., 6, 1-16.